

Correlating Structure and Stability of DNA Duplexes with Incorporated 2'-O-Modified RNA Analogues^{†,‡}

Valentina Tereshko,[§] Stefan Portmann,^{||} Edward C. Tay,[⊥] Pierre Martin,[#] François Natt,[#] Karl-Heinz Altmann,^Δ and Martin Egli^{*,§}

Drug Discovery Program and Department of Molecular Pharmacology and Biological Chemistry, Northwestern University Medical School, Chicago, Illinois 60611-3008, Department of Informatics, ETH-Zentrum, CH-8092 Zürich, and Swiss Center for Super Computing, CH-6928 Manno, Switzerland, School of Engineering, Northwestern University, Evanston, Illinois 60208, and Core Technologies Area and Therapeutic Area Oncology, Novartis Pharma Inc., CH-4002 Basel, Switzerland

Received February 19, 1998; Revised Manuscript Received May 13, 1998

ABSTRACT: Chemically modified nucleic acids are currently being evaluated as potential antisense compounds for therapeutic applications. 2'-O-Ethylene glycol substituted oligoribonucleotides are second-generation antisense inhibitors of gene expression with promising features for in vivo use. Relative to DNA, they display improved RNA affinity and higher nuclease resistance. Moreover, chimeric oligonucleotides with 2'-O-methoxyethyl ribonucleoside wings and a central DNA phosphorothioate window have been shown to effectively reduce the growth of tumors in animal models at low doses. Using X-ray crystallography, we have determined the structures of three A-form DNA duplexes containing the following 2'-O-modified ribothymidine building blocks: 2'-O-methoxyethyl ribo-T, 2'-O-methyl[tri(oxyethyl)] ribo-T, and 2'-O-ethoxymethylene ribo-T. In contrast to 2'-O-ethylene glycol substituents, the presence of a 2'-O-ethoxymethylene group leads to slightly reduced RNA affinity of the corresponding oligonucleotides. The three structures allow a qualitative rationalization of the differing stabilities of duplexes between oligonucleotides comprising these types of 2'-O-modified ribonucleotides and complementary RNAs. The stabilizing 2'-O-ethylene glycol substituents are conformationally preorganized for the duplex state. Thus, the presence of one or several ethylene glycol moieties may reduce the conformational space of the substituents in an oligonucleotide single strand. In addition, most of these preferred conformations appear to be compatible with the minor groove topology in an A-type duplex. Factors that contribute to the conformational rigidity of the 2'-O-substituents are anomeric and gauche effects, electrostatic interactions between backbone and substituent, and bound water molecules.

DNA and RNA oligonucleotides are rapidly degraded under physiological conditions by a variety of exo- and endonucleases. As part of the search for antisense oligonucleotides with improved efficacy for therapeutic applications, a multitude of chemically modified nucleic acids has been explored in recent years (1–5). Important criteria for judging the practical aptness of a particular modification are RNA affinity and binding selectivity of the corresponding oligonucleotides (5, 6–9). The former should be considerably enhanced relative to DNA, and the latter must be maintained.

Among the available sites for modifications, the furanose 2'-position has been demonstrated to offer several advantages. (1) 2'-Modification can confer improved nuclease resistance

(10, 11). (2) 2'-Heteroatom substituents can promote an RNA-like C3'-endo sugar conformation in an analogue. This should preorganize the modified oligonucleotide for the conformation adopted by the strands in an A-form RNA duplex (5, 12, 13). (3) As a result, 2'-O-modification can lead to substantially increased stability of duplexes between modified strands and their RNA complements. This is consistent with the higher stability of RNA duplexes relative to DNA–RNA hybrids (14, 15). Thus, 2'- α -fluoro substitution of oligodeoxyribonucleotides increases the T_m of the corresponding DNA–RNA duplexes by around 2.5 °C per modified residue but does not provide sufficient nuclease resistance for in vivo applications (16, 17, and references cited therein). Similarly, the 2'-O-methyl modification results in enhanced RNA affinity (18–21) but furnishes only a moderate improvement in nuclease resistance (Figure 1).

Attachment of longer aliphatic chains to the 2'-oxygen of the ribose moiety improves nuclease resistance but has deleterious effects on duplex stability (22). For example, incorporation of 2'-O-nonyl-modified residues into DNA lowers the UV melting temperature of the corresponding DNA–RNA duplexes by 2–3 °C per modification. In an even more dramatic fashion, oligonucleotides with 2'-O-[(*t*-Bu)Me₂Si] substitutions reduce DNA–RNA duplex stability with a ΔT_m of ca. 7 °C per modification (S. M. Freier, personal

[†] Supported by the National Institutes of Health (Grant R01 GM-55237).

[‡] The coordinates for the three structures have been deposited in the Nucleic Acid Database [entry codes AH0002 (EOM), AH0003 (MOE), and AH0004 (TOE)].

* To whom correspondence should be addressed: phone (312) 503-0845; fax (312) 503-0796; e-mail m-egli@nwu.edu.

[§] Northwestern University Medical School.

^{||} ETH-Zentrum and Swiss Center for Super Computing.

[⊥] Northwestern University.

[#] Core Technologies Area, Novartis Pharma Inc.

^Δ Therapeutic Area Oncology, Novartis Pharma Inc.

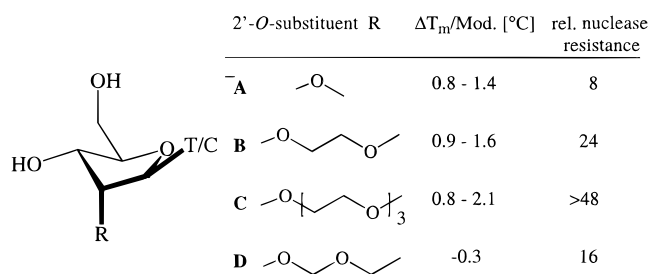


FIGURE 1: Structure, modified DNA–RNA duplex stability, and relative nuclease resistance of 2'-O-modified RNA analogues: (A) 2'-O-methyl, (B) 2'-O-methoxyethyl (MOE), (C) 2'-O-methyl[tri(oxyethyl)] (TOE), and (D) 2'-O-ethoxymethylene (EOM). The changes in melting temperature ($\Delta T_m/\text{mod.}$) relative to the unmodified DNA–RNA duplexes were compiled from UV melting data for hybridizations between DNA oligonucleotides containing either a single 2'-O-modified ribothymidine or consecutive stretches of 2'-O-modified residues (T, C, or 5-MeC) and complementary RNAs in various buffers (21). The relative nuclease resistances, using the corresponding unmodified oligodeoxyribonucleotide as the standard (relative stability = 1), were assayed in 10% heat-denatured calf fetal serum (21, 24).

communication). Finally, terminal branching in the case of the 2'-O-allyl modification results in the complete loss of RNA affinity, although the allyl group itself improves hybridization to RNA (23).

Surprisingly, certain 2'-O-alkoxyalkyl substituents were found to affect RNA binding favorably, even when the side chain features 10 non-hydrogen atoms (Figure 1, 2'-O-methyl[tri(oxyethyl)] ribonucleoside = TOE) (3, 21, 24). However, significantly enhanced RNA binding affinity is also conferred by a single ethylene glycol unit attached to the 2'-position and, in addition, provides considerably more protection against nuclease degradation than the 2'-O-methyl modification (Figure 1, 2'-O-methoxyethyl ribonucleoside = MOE). Furthermore, introduction of branched 2'-O-alkoxyalkyl substituents, for example, a glycerol moiety, further improves the stability of duplexes between modified DNA strands and RNA (3, 21, 24). Shifting the position of the second oxygen atom within the substituent away from the β -position affects duplex formation with complementary RNA in a negative fashion (Figure 1, 2'-O-ethoxymethylene ribonucleoside = EOM). It appears that favorable effects on RNA binding can only be achieved if the oxygen atoms in the alkoxyalkyl side chain are separated by an ethylene spacer. Due to the gauche effect, the conformation of the C–C torsion in the ethylene group is then limited to either $-sc$ or $+sc$. The resulting higher conformational rigidity of the 2'-O-alkoxyalkyl group relative to a long unstructured alkyl chain could provide an entropic advantage for duplex formation, provided the set of stabilized conformations is compatible with the duplex topology.

2'-O-MOE antisense oligonucleotides, including gapmers with central DNA phosphorothioate windows (6, 25, 26), have been tested against a number of targets in *in vitro* cell-based assays as well as in animal models (7, 24, 27). The results obtained thus far render the 2'-O-alkoxyalkyl RNA analogues very promising second-generation antisense compounds for therapeutic applications.

To gain insight into the conformational properties of the alkoxyalkyl substituents as part of a modified DNA–RNA duplex and also to more clearly define the parameters contributing to their favorable effects on duplex stability,

we have crystallized self-complementary modified DNA duplexes with the sequence 5'-d(GCGTAtACGC), containing different types of 2'-O-alkoxyalkyl residues ($t = 2'$ -O-MOE, 2'-O-TOE, or 2'-O-EOM ribothymidine). In the crystals, all three duplexes adopt A-form geometry. Because the conformation of duplexes between RNA and 2'-O-modified RNA strands is most likely also of the A-type, our structures constitute a proper template for studying these modifications. Here, we report details of these crystal structures at resolutions between 1.65 and 1.93 Å and attempt to correlate the observed thermodynamic stability data with conformational properties of the modified residues and duplexes as well as the changes in hydration produced by the different 2'-O-substituents.

METHODS

Selection of Modification Site and Crystallization. The DNA decamer GCGTATACGC had previously been used as a template to study the conformational properties of chimeric DNA–RNA oligonucleotides (28), an Okazaki fragment (29), the 2'-O-methyl ribonucleoside modification (30), and single-base bulges (31). In the case of 2'-O-methyl RNA, crystals of the decamer had been obtained with the modified building block incorporated at position 5. Therefore, a decamer was synthesized with 2'-O-MOE ribadenosine also at position 5. However, all attempts to crystallize the resulting duplex failed, and two additional oligonucleotides were produced, one with G3 replaced by MOE-rG and the other with T6 replaced by MOE-rT. Well-diffracting crystals were only obtained of the latter (MOE decamer). Consequently, DNA decamers with the TOE and EOM modifications at T6 were also synthesized and crystallized (TOE and EOM decamers, respectively). All modified oligonucleotides were synthesized with the standard phosphoramidite method on a 3.5 μmol scale, according to previously described procedures (21). After deprotection, the trityl-on strands were purified by RP-HPLC, using a Rainin C4 column with 0.05 M TEAA buffer, pH 7, and acetonitrile as the eluent. Following detritylation, the strands were HPLC-purified a second time, and after desalting and lyophilization, the concentrations of aqueous stock solutions were adjusted to between 5 and 10 mM. The three modified oligonucleotides GCGTAtACGC were crystallized as follows. MOE decamer: hanging drop method; 0.8 mM oligonucleotide, 25 mM sodium cacodylate, pH 6.0, 7.5 mM magnesium acetate, and 850 mM ammonium sulfate, equilibrated against 50 mM sodium cacodylate, pH 6.0, 15 mM magnesium acetate, and 1.7 M ammonium sulfate. TOE decamer: sitting drop method; 1.2 mM oligonucleotide, 30 mM sodium cacodylate, pH 6.3, 8 mM magnesium chloride, and 20 mM spermine tetrahydrochloride, equilibrated against 40% (v/v) 2-methyl-2,4-pentanediol (MPD). EOM decamer: hanging drop method; 1.2 mM oligonucleotide, 20 mM sodium cacodylate, pH 6.0, 40 mM sodium chloride, 6 mM spermine tetrahydrochloride, 10 mM barium chloride, and 5% MPD, equilibrated against 35% MPD. With each of the duplexes, isomorphous crystals could be obtained under several other conditions.

Data Collection and Structure Refinement. For the MOE decamer, diffraction data were collected at room temperature by sealing a crystal together with a droplet of mother liquor into a thin-walled glass capillary. Crystals of the TOE and

Table 1: Selected Crystal and Refinement Data

decamer	MOE	TOE	EOM
cell constants (Å)	$a = 24.93$ $b = 44.59$ $c = 45.38$	$a = 24.64$ $b = 43.62$ $c = 45.47$	$a = 24.62$ $b = 44.08$ $c = 46.18$
crystal system	orthorhombic	orthorhombic	orthorhombic
space group	$P2_12_12_1$	$P2_12_12_1$	$P2_12_12_1$
temperature (°C)	room	-170	-170
max resolution (Å)	1.93	1.65	1.60
unique reflections ($F > 2\sigma(F)$, 8 Å max)	3757	5915	6414
completeness (%) [$F > 2\sigma(F)$, 8 Å max]	93.1	96.3	92.0
final R -factor (%) ^a	16.8	18.9	15.9
final R -free (%) ^{a,b}	21.0	22.0	18.4
water molecules	58	105	140
ions		2 Mg ²⁺	1 spermine ⁴⁺
rms bond lengths (Å)	0.009	0.009	0.007
rms bond angles (deg)	1.30	1.36	1.21

^a Multiscale procedure, 10 bins. ^b Using a 10% subset.

EOM decamers were picked up from their droplets with a nylon loop and directly transferred into a cold nitrogen stream (-170 °C). All data were collected on a Rigaku R-AXIS-IIc image plate system, mounted on a rotating anode X-ray generator. Various detector-crystal distances, oscillation angles, and exposure times were used. Data were processed with the DENZO/SCALEPACK program package in all cases (32). Selected crystal data as well as diffraction data and refinement statistics are summarized in Table 1. The structures were solved by the molecular replacement method, using the program AMORE (33) and a standard A-DNA duplex as the search model. The structures were refined with the program X-PLOR (34) with the most recent parameter and topology files (35), expanded by newly defined patches for the three 2'-*O*-modified RNA residues. Resolutions, refinement parameters, and final R -factors for the three structures are listed in Table 1, and examples of the qualities of final omit electron density maps are depicted in Figure 2.

RESULTS AND DISCUSSION

Overall Features of the Modified Decamer Duplexes. In all three crystals, the duplexes adopt A-form geometry, but only the structures of the TOE and EOM decamers are isomorphous. Their overall conformations differ only minimally, and the lattice interactions comprise stacking of terminal base pairs into the minor grooves of neighboring duplexes, typical for A-DNA crystals (36). The ribose moieties of modified residues display typical C3'-*endo* puckers. Average helical parameters for the three duplexes and an unmodified chimeric DNA-RNA hybrid duplex with identical sequence are listed in Table 2.

The resolutions of all three structures are better than 2 Å. It is noteworthy that flash-freezing in the case of the TOE and EOM decamer crystals led to an improvement of resolution by around 0.3 Å relative to the MOE structure, for which data were collected at room temperature (Table 1). For each structure, the 2'-*O*-substituents are well defined in the electron density maps, and there is no apparent disorder in any of them (Figure 2). The areas in the vicinity of the modification sites are not severely constrained by packing contacts. Thus, despite the relatively dense packing and low water content displayed by the orthorhombic oligonucleotide

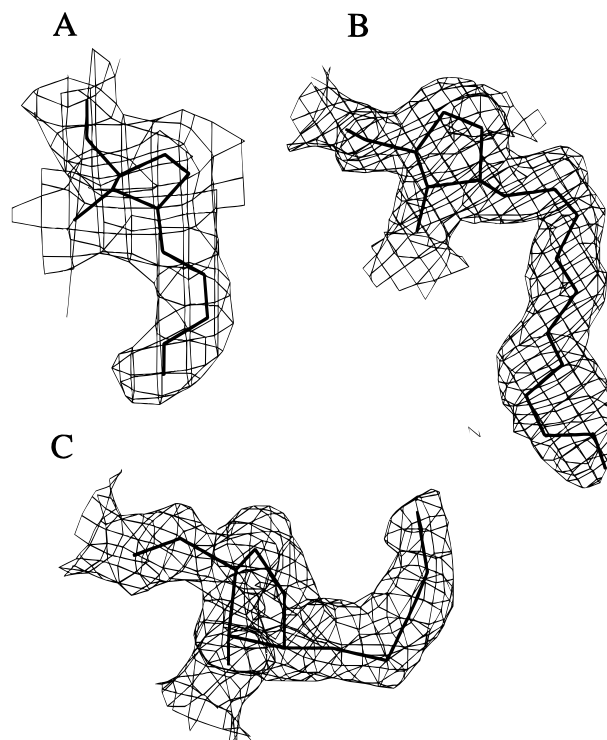


FIGURE 2: Final ($2F_o - F_c$) omit electron density maps (0.8σ level) around the sugar portion of modified residues: (A) MOE decamer (T16), (B) TOE decamer (T6), and (C) EOM decamer (T6).

crystals, the conformations of the 2'-*O*-substituents are clearly not induced by lattice forces.

Conformational Features of the 2'-*O*-MOE Substituent. Atoms in the three 2'-*O*-substituents have been numbered alphabetically. For the MOE substituent, O2' is bound to CA', which is followed by CB', OC', and CD' (Figure 1A). The geometries of the MOE substituents in the two modified residues are similar. The only significant deviation occurs for the torsion angle around the O2'-CA' bond (Figure 3A, Table 3). In residue T6, the conformation of this torsion falls in the negative anticlinal ($-ac$) range. The conformation of the corresponding angle in residue T16 lies in the antiperiplanar (ap) range. As a consequence of the gauche effect, the conformation around the C-C bond of the central ethyl linker falls into a synclinal (sc) range; for both T6 and T16, it is $-sc$. The other shared feature among all substituents, with one exception (see EOM paragraph), is the ap conformation of the C3'-C2'-O2'-CA' torsion angle (Table 3). This feature was also observed in the structure of a DNA duplex with incorporated 2'-*O*-methyl RNA building blocks (30) and in the recent crystal structure of a uniformly 2'-*O*-methyl-modified RNA duplex (39). The orientation around the C2'-O2' bond is most likely sterically controlled.

The 2'-*O*-MOE substituents in the modified base pair step protrude into the minor groove (Figure 3A). The conformations around individual bonds produce an overall orientation of the MOE substituents that is approximately perpendicular to the helical axis (Figure 4). Thus, the expected, relative to a butyl group, higher conformational rigidity of the 2'-*O*-MOE substituent is largely borne out by the crystal structure. However, an additional factor may contribute to the conformational rigidity of the MOE substituents. Both, residue T6 and T16, feature a water molecule that is located between the 2'-*O*-substituent and the backbone 3'-oxygen

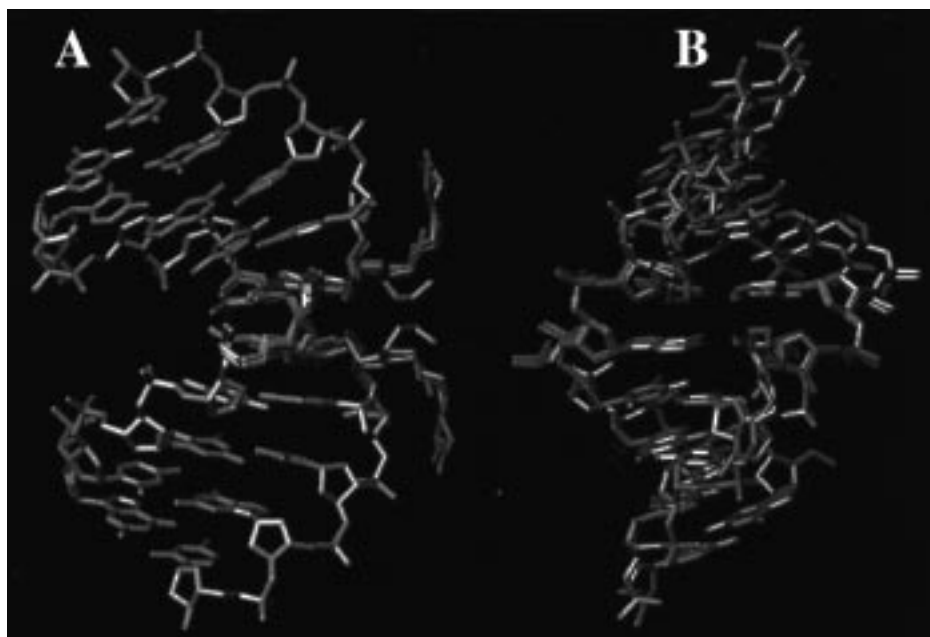


FIGURE 4: Superposition of the central base pair step from the MOE and TOE decamer duplexes within the framework of the MOE decamer duplex. (A) View across the major and minor grooves, roughly along the long dimension of the central base pairs. (B) View into the minor groove, roughly along the local pseudo-2-fold rotation axis of the central base pair step. To convey an optimal impression of the conformational variations displayed by the 2'-*O*-substituents, the base pair steps were rotated around their local pseudo-2-fold rotation axes, thus creating superpositions of all four substituents on either border of the minor groove. The A5pT6 and modeled A15pT16 base steps carrying the 2'-*O*-substituents of residues MOE T6 and TOE T6 are shown in cyan and red, respectively. The A15pT16 and modeled A5pT6 base steps carrying the 2'-*O*-substituents of residues MOE T16 and TOE T16 are shown in green and pink, respectively.

Table 3: Values of Torsion Angles in the 2'-*O*-Substituents

torsion angle (deg)	MOE T6	MOE T16	TOE T6	TOE T16	EOM T6	EOM T16
O4'-C1'-C2'-O2'	89	90	89	90	88	90
O3'-C3'-C2'-O2'	45	46	45	45	43	42
C1'-C2'-O2'-CA'	70	71	68	63	71	130
C3'-C2'-O2'-CA'	-179	-179	179	173	-179	-120
C2'-O2'-CA'-CB'	-129	-174	171	166		
C2'-O2'-CA'-OB'					-90	-82
O2'-CA'-CB'-OC'	-34	-49	-42	-55		
O2'-CA'-OB'-CC'					-67	-177
CA'-CB'-OC'-CD'	-74	-88	-169	146		
CA'-OB'-CC'-CD'					143	178
CB'-OC'-CD'-CE'			-177	178		
OC'-CD'-CE'-OF'			-95	-56		
CD'-CE'-OF'-CG'			159	-161		
CE'-OF'-CG'-CH'			163	-137		
OF'-CG'-CH'-OI'			9	-55		
CG'-CH'-OI'-CK'			165	-10		

Conformational Features of the 2'-*O*-TOE Substituent. As is the case for the shorter MOE group, the conformations around the C-C bonds of the ethyl linkers in the TOE substituents of both modified residues all fall into the *sc* range (Figure 3B, Table 3). Five of these bonds adopt *-sc* conformation, and only for the one in residue T6 which is most remote from O2' the conformation is *+sc*. All other torsion angles within the TOE substituent of residue T6 lie in the *ap* range. For residue T16, five of the non-C-C torsion angles assume *ap* conformations, while the conformations around the OF'-CG' and CH'-OI' bonds fall into the *-ac* and *-sc* ranges, respectively. As observed with the MOE substituent, the well-defined appearance of the TOE substituents in the electron density maps (Figure 2B) and the conserved gauche conformations of the ethyl linkers are consistent with a higher rigidity of the PEG-like substituent compared with an aliphatic side chain of similar length.

Table 4: Lengths of Hydrogen Bonds between Water Molecules and Oxygen Atoms of 2'-*O*-Substituents as Well as the 3'-Oxygen from 2'-*O*-Modified Residues

donor (residue)	acceptor (residue)	distance (Å)
W (150)	MOE decamer	
	O3' (T6)	3.03
	O2' (T6)	3.09
W (158)	OC' (T6)	3.28
	O3' (T16)	2.88
	O2' (T16)	3.17
	OC' (T16)	3.07
W (110)	TOE decamer	
	O3' (T6)	3.21
	O2' (T6)	2.99
W (178)	OC' (T6)	3.10
	OF' (T6)	3.42
	OI' (T6)	3.44
W (151)	O3' (T16)	3.19
	O2' (T16)	3.19
W (214)	EOM decamer	
	O3' (T6)	3.19
W (140)	O2' (T6)	3.39
	OB' (T6)	2.84
	O2 (T16)	2.78

Rather than protruding into the minor groove, perpendicular to the helical axis, the TOE substituents follow the direction of the duplex backbones in a 5' → 3' manner (Figures 3B and 4). Notwithstanding a number of differences in the torsion angles within the TOE substituents of residues T6 and T16, the relative orientations of the backbone and substituent are similar in both cases. Closer inspection of the conformations of the TOE substituents of T6 and T16 reveals that these are largely governed by electrostatic forces between oxygen atoms of the 2'-*O*-substituent and C-H groups of the deoxyribose from the 3'-adjacent residues A7 and A17, respectively (Figure 5). While one of the electron

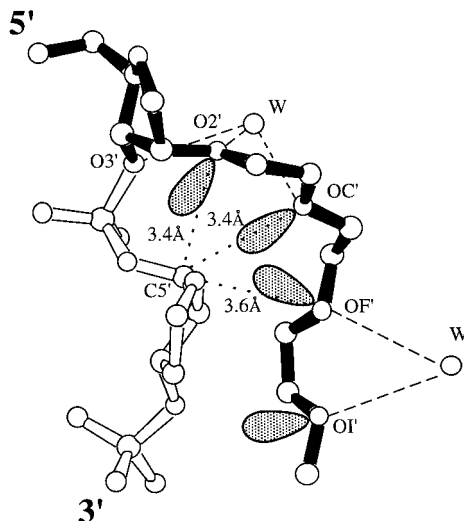


FIGURE 5: Close-up view of the electrostatic interactions between oxygen atoms from the 2'-*O*-substituent of residue TOE T6 (top, solid bonds) and deoxyribose C-H groups of the adjacent residue A7 (bottom). Selected oxygen and carbon atoms are labeled, water molecules are shown as open spheres, lone electron pairs of TOE oxygen atoms directed toward the duplex backbone are stippled, C5'-H5'...O (TOE) interactions are shown as dotted lines, and water...O (TOE) hydrogen bonds are shown as dashed lines.

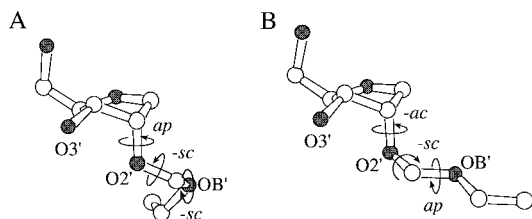


FIGURE 6: Conformations of the 2'-*O*-EOM substituent: (A) residue T6 and (B) residue T16. The conformations of selected torsion angles are depicted; the conformation around the C2'-O2' bond refers to the C3'-C2'-O2'-CA' torsion. Oxygen atoms are stippled in gray and are labeled.

lone pairs of each oxygen atom in the substituent is directed toward the sugar moiety, the other is used for hydrogen bonding to water molecules (Figures 3B and 5).

Two water molecules are bound to the TOE substituent of residue T6. The binding mode for the first one closely resembles that observed with the MOE substituents (Figure 3A,B, Table 4), while the second is involved in hydrogen bonding to the additional oxygen atoms OF' and OI' present in the TOE group. Only one water molecule is bound to the substituent of residue T16, with close contacts being formed to O3' and O2' (Figure 3B, Table 4). In summary, the conformational features of the 2'-*O*-TOE substituent are thus determined by three different parameters: gauche effects between its oxygen atoms, electrostatic interactions between substituent and backbone, and bound water molecules.

Conformational Features of the 2'-*O*-EOM Substituent. In the EOM substituent, O2' and the second oxygen atom are separated by a methylene rather than an ethyl group (Figure 1). Thus, the conformations around the O2'-CA' and CA'-OB' bonds would be expected to be limited by an anomeric effect and should lie in the +*sc* or -*sc* ranges. This is indeed the case for the EOM substituent of residue T6 (Figure 6A, Table 3) but not for the one of residue T16 which assumes an almost extended arrangement (Figure 6B). Only the conformation of the torsion angle around the O2'-CA' bond

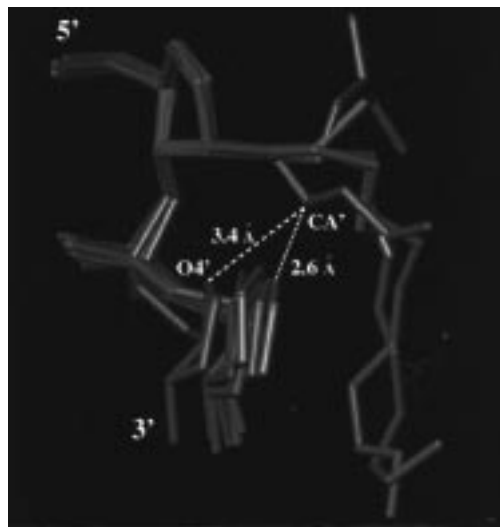


FIGURE 7: Superposition of all 2'-*O*-substituents from the MOE, TOE, and EOM decamer duplex structures as well as the corresponding region of the unmodified duplex [r(GCG)d(TATACGC)]₂ (37), performing a best fit for the sugar atoms of residues T6 and T16 (top). The comparison illustrates the conformational shift of the 3'-adjacent residue as a consequence of the extended conformation of the 2'-*O*-substituent in the case of residue EOM T16 (green). The dinucleotide step EOM T6pA7 is shown in cyan, the dinucleotide steps of the MOE and TOE structures are shown in gray, and the corresponding steps in the unmodified DNA-RNA chimeric duplex are shown in red. The observed contact between CA' (T16) and O4' (A17) and the hypothetical short contact that would occur without the shift are highlighted as dashed lines, and the corresponding distances are given.

lies in the *sc* range, while the CA'-OB' bond is found in an *ap* conformation.

The poorer hydration of the EOM substituents, compared with both MOE and TOE, provides good evidence that the length of the spacer between oxygen atoms critically affects the level of hydration (Figure 3C). The ethyl group allows the oxygen atoms to bind water in a cooperative fashion. By comparison, only two water molecules are found in the vicinity of the 2'-*O*-EOM substituents. The water molecule that is bound to the O2' and O3' atoms of residue T6 appears only weakly occupied (Figure 3C). Binding of the second water molecule requires the involvement of the exocyclic carbonyl 2-oxygen of T16.

While the conformations of the other 2'-*O*-substituents are compatible with a standard A-type duplex geometry, the particular conformation assumed by the EOM substituent of residue T16 results in a local geometrical distortion of the modified duplex. In addition to not conforming to the anomeric effect, the torsion angle C3'-C2'-O2'-CA' of this modified residue differs by around 60° from the *ap* conformation displayed by all other 2'-*O*-substituted sugar moieties (Table 3). Comparison of selected helical parameters in the vicinity of the modified residues for the three duplexes reveals that the arrangement of the EOM substituent of residue T16 produces a substantial shift of the adjacent residue A17 into the minor groove (Figure 7, Table 2). Thus, the helical twist between base pairs A5•T16 and T4•A17 is reduced by roughly 10° relative to the value in a standard A-type duplex. Although the MOE and TOE decamer duplexes also show somewhat reduced twists at this site, the reduction is larger for the EOM decamer and amounts to more than twice the standard deviation of twist values in all

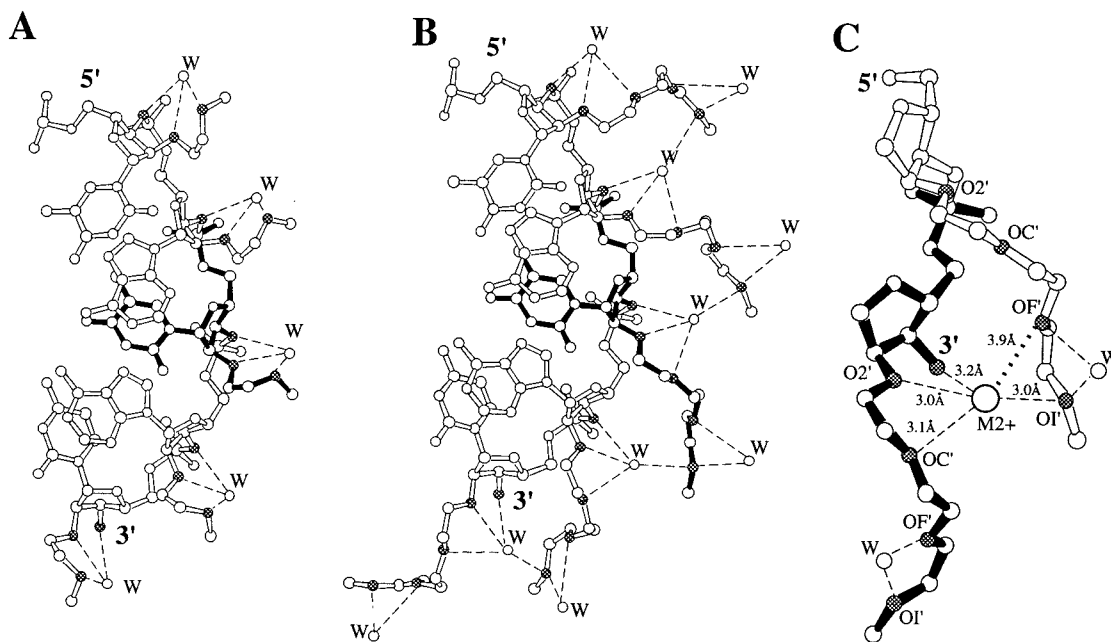


FIGURE 8: Models of consecutive stretches of (A) 2'-O-MOE RNA and (B) 2'-O-TOE RNA based on the conformations of residues MOE T6 and TOE T6 (solid bonds) in the corresponding decamer duplexes. 3'-Oxygen atoms and oxygen atoms from the substituents are highlighted, water molecules are drawn as open spheres, and hydrogen bonds are shown by dashed lines. Both ribose modifications are likely to result in improved backbone hydration compared with DNA, and in the case of 2'-O-TOE RNA, substituents from adjacent residues may provide a binding site for mono- or divalent metal cations. (C) Close-up view of the relative orientation of adjacent 2'-O-TOE RNA residues based on the conformation of the 2'-O-substituent of residue TOE T6 (solid bonds). Individual substituents provide binding sites for two water molecules, the first involving oxygen atoms O3', O2', and OC' and the second OF' and OI'. However, for a modified dinucleotide step, the latter two atoms from the 5'-residue and the former three from the 3'-residue may provide a crown ether-like binding pocket for metal cations.

nine base pair steps (data not shown). 2'-O-EOM-modified strands display lower RNA affinity than the corresponding DNA oligonucleotides (21). Thus, we are able to link the unfavorable thermodynamic effects of this modification to a particular conformation of the 2'-O-substituent in the crystal structure that results in a distorted duplex geometry.

Consecutive Stretches of 2'-O-MOE and 2'-O-TOE RNA. Our structures provide information about the conformational properties as well as hydration of isolated 2'-O-modified RNA residues in a A-form duplex environment. To gain insight into potential structural or stability features of stretches of modified residues with A-type backbone conformation, we have generated models of fully modified pentamers, based on the conformations of the 2'-O-MOE and 2'-O-TOE substituents of residues T6, respectively (Figure 8). The models are based on the assumption that a hybrid duplex between an RNA strand and a 2'-O-modified oligoribonucleotide would most likely assume A-form geometry.

In the case of the MOE modification, our model suggests that there are no interactions between substituents from adjacent residues (Figure 8A). Furthermore, the distances between substituent oxygen atoms from such residues are too long to be bridged by single water molecules. However, we cannot exclude the possibility that bridges formed by two or more water molecules could be stabilized by substituents of adjacent residues.

A different picture emerges for the 2'-O-TOE modification. In the model, the oxygen atoms of substituents from modified residues are spaced closely enough to form a binding site for either water molecules or metal cations (Figure 8B). It should be stressed that, as in the case of DNA, the 2'-O-modified RNA backbone remains deficient in potential

hydrogen bond donors. UV melting data for hybrid duplexes between RNA and 2'-O-TOE oligoribonucleotides in near-physiological buffer solution (moderate amounts of Mg^{2+} and spermine) have shown unusually high nonadditive gains in thermal stability relative to the corresponding DNA-RNA hybrids (21). Our model demonstrates that the TOE substituents of adjacent modified residues in concert could provide binding sites for mono- or divalent metal cations (Figure 8C). The observed stability improvement could then be rationalized in terms of a neutralization of the backbone due to the close vicinity of cations and phosphate groups.

Conclusions. All clinical trials currently ongoing with antisense compounds are conducted with 2'-deoxy phosphorothioates (42–45). Although initial results are encouraging, phosphorothioates clearly suffer from suboptimal RNA binding (5, 7, 24) as well as a number of pharmacokinetic, pharmacodynamic, and toxicological limitations (8, 46–48).

Several features of the 2'-O-methoxyethyl substituent render it a promising modification for the design of second-generation antisense oligonucleotides with reduced thioate content. Relative to DNA, the corresponding oligonucleotides display improved RNA affinity. The average gain of 1.4 °C per modification in T_m for hybridization to RNA translates into a reduction of 4 orders of magnitude in the dissociation constant for a modified 20-mer with 2'-O-MOE ribonucleotides in its wings and a 6-mer 2'-deoxy phosphorothioate gap in the middle. Along with the higher affinity, 2'-O-MOE RNA exhibits equal or improved pairing specificity compared with DNA (21). By acting via a steric block mechanism, oligonucleotides that hybridize to RNA with high stability can overcome the necessity to induce RNase H-mediated degradation of the target sequence. Thus, a fully

2'-*O*-MOE-modified 20-mer was shown to reduce ICAM-1 expression in an RNase H-independent fashion with higher efficiency than the corresponding DNA phosphorothioate when targeted against the 5'-cap region of human ICAM-1 RNA in HUVEC cells (49). The potential of the 2'-*O*-MOE RNA modification was also demonstrated by effectively reducing the growth of tumors in animal models with 2'-*O*-MOE RNA/2'-deoxy phosphorothioate gapmers, targeted to either C-raf kinase or PKC- α RNA (7, 24).

In light of the MOE, TOE, and EOM decamer crystal structures, the thermodynamic stability data for duplexes between RNA and 2'-*O*-alkoxyalkyl-modified RNA analogues can be rationalized as follows. The stabilizing 2'-*O*-MOE and 2'-*O*-TOE substituents as well as the modified furanose ring (C3'-*endo* pucker) are conformationally preorganized for an A-form duplex. In accordance with the gauche effect, the conformations of the torsion angles around the ethyl C-C bonds in the 2'-*O*-substituents fall into the *sc* ranges in every case. The resulting arrangements are compatible with the minor groove topology in an A-form duplex. The conformations of the substituents are further constrained by the coordination of water molecules. A particular mode of hydration that involves O3' and O2' is conserved in five of the six substituents studied in the crystallographic context. In terms of hydrogen-bonding enthalpy, the observed hydration of the 2'-*O*-MOE and 2'-*O*-TOE substituents distinguishes them sharply from destabilizing aliphatic 2'-*O*-substituents, in particular when considering the conserved water binding site (22). The structure of the TOE decamer has revealed a further stabilizing feature, namely, a network of C-H \cdots O hydrogen bonds between substituent and backbone, not unlike the one found between the backbones of adjacent duplexes in a recent crystal structure of *cis*-platin bound to B-DNA (50). The T_m difference for pairing between an RNA and a modified DNA strand, the latter containing either 2'-*O*-MOE or 2'-*O*-EOM ribonucleotides, amounts to almost 2 °C per modification (21). The crystal structure of the EOM decamer demonstrates the reduced conformational preorganization of the 2'-*O*-EOM substituent compared with the 2'-*O*-MOE and 2'-*O*-TOE substituents. Moreover, the particular arrangement of one of the 2'-*O*-EOM substituents leads to a local duplex deformation. Thus, the three crystal structures provide satisfactory qualitative interpretations of the observed thermodynamic stability data.

ACKNOWLEDGMENT

We are indebted to Northwestern University Medical School for supporting structural research through the Macromolecular Crystallography and Biochemical Computation Resource.

REFERENCES

- Manoharan, M. (1993) in *Antisense Research and Applications* (Crooke, S. T., and Lebleu, B., Eds.) pp 303–349, CRC Press, Boca Raton, FL.
- Sanghvi, Y. S., and Cook, P. D., Eds. (1994) *Carbohydrate Modifications in Antisense Research*, ACS Symposium Series No. 580, American Chemical Society, Washington, DC.
- De Mesmaeker, A., Häner, R., Martin, P., and Moser, H. E. (1995) *Acc. Chem. Res.* 28, 366–374.
- De Mesmaeker, A., Altmann, K.-H., Waldner, A., and Wendeborn, S. (1995) *Curr. Opin. Struct. Biol.* 5, 343–355.
- Freier, S. M., and Altmann, K.-H. (1997) *Nucleic Acids Res.* 25, 4429–4443.
- Monia, B. P., Lesnik, E. A., Gonzalez, C., Lima, W. F., McGee, D., Guinosso, C. J., Kawasaki, A. M., Cook, P. D., and Freier, S. M. (1993) *J. Biol. Chem.* 268, 14514–14522.
- Altmann, K.-H., Fabbro, D., Dean, N. M., Geiger, T., Monia, B. P., Müller, M., and Nicklin, P. (1996) *Biochem. Soc. Trans.* 24, 630–637.
- Crooke, S. T., Graham, M. J., Zuckerman, J. E., Brooks, D., Conklin, B. S., Cummins, L. L., Greig, M. J., Guinosso, C. J., Kornbrust, D., Manoharan, M., Sasmor, H. M., Schleich, T., Tivel, K. L., and Griffey, R. H. (1996) *J. Pharmacol. Exp. Ther.* 277, 923–937.
- Egli, M. (1998) in *Advances in Enzyme Regulation* (Weber, G., Ed.) pp 181–203, Vol. 38, Elsevier, Oxford, U.K.
- Cummins, L. L., Owens, S. R., Risen, M. L., Lesnik, E. A., Freier, S. M., McGee, D., Guinosso, C. J., and Cook, P. D. (1995) *Nucleic Acids Res.* 23, 2019–2024.
- Griffey, R. H., Monia, B. P., Cummins, L. L., Freier, S. M., Greig, M. J., Guinosso, C. J., Lesnik, E. A., Manalili, S. M., Mohan, V., Owens, S., Ross, B. R., Sasmor, H., Wancewicz, E., Weiler, K., Wheeler, P. D., and Cook, P. D. (1996) *J. Med. Chem.* 39, 5100–5109.
- Egli, M. (1996) *Angew. Chem., Int. Ed. Engl.* 35, 1894–1909.
- Herdewijn, P. (1996) *Liebigs Ann. Chem.*, 1337–1348.
- Hall, K. B., and McLaughlin, L. W. (1991) *Biochemistry* 30, 10606–10613.
- Lesnik, E. A., and Freier, S. M. (1995) *Biochemistry* 34, 10807–10815.
- Kawasaki, A. M., Casper, M. D., Freier, S. M., Lesnik, E. A., Zounes, M. C., Cummins, L. L., Gonzalez, C., and Cook, P. D. (1993) *J. Med. Chem.* 36, 831–841.
- Schultz, R. G., and Gryaznov, S. M. (1996) *Nucleic Acids Res.* 24, 2966–2973.
- Inoue, H., Hayase, Y., Imura, A., Iwai, S., Miura, K., and Ohtsuka, E. (1987) *Nucleic Acids Res.* 15, 6131–6148.
- Sproat, B. S., and Lamond, A. I. (1991) in *Proceedings of the EMBL Conference on Oligonucleotide Analogs* (Eckstein, F., Ed.) pp 49–86, IRL Press, Heidelberg, Germany.
- Lamond, A. I., and Sproat, B. S. (1993) *FEBS Lett.* 325, 123–127.
- Martin, P. (1995) *Helv. Chim. Acta* 78, 486–504.
- Lesnik, E. A., Guinosso, C. J., Kawasaki, A. M., Sasmor, H., Zounes, M., Cummins, L. L., Ecker, D. J., Cook, P. D., and Freier, S. M. (1993) *Biochemistry* 32, 7832–7838.
- Ibarren, A. M., Sproat, B. S., Neuner, P., Sulston, I., Ryder, U., and Lamond, A. I. (1990) *Proc. Natl. Acad. Sci. U.S.A.* 87, 7747–7751.
- Altmann, K.-H., Dean, N. M., Fabbro, D., Freier, S. M., Geiger, T., Häner, R., Hüskén, D., Martin, P., Monia, B. P., Müller, M., Natt, F., Nicklin, P., Phillips, J., Pieles, U., Sasmor, H., and Moser, H. E. (1996) *Chimia* 50, 168–176.
- Cook, P. D. (1991) *Anti-Cancer Drug Des.* 6, 585–607.
- Cook, P. D. (1993) in *Antisense Research and Applications* (Crooke, S. T., and Lebleu, B., Eds.) pp 149–187, CRC Press, Boca Raton, FL.
- Altmann, K.-H., Martin, P., Dean, N. M., and Monia, B. P. (1997) *Nucleosides Nucleotides* 16, 917–926.
- Egli, M., Usman, N., and Rich, A. (1993) *Biochemistry* 32, 3221–3237.
- Egli, M., Usman, N., Zhang, S., and Rich, A. (1992) *Proc. Natl. Acad. Sci. U.S.A.* 89, 534–538.
- Lubini, P., Zürcher, W., and Egli, M. (1994) *Chem. Biol.* 1, 39–45.
- Portmann, S., Grimm, S., Workman, C., Usman, N., and Egli, M. (1996) *Chem. Biol.* 3, 173–184.
- Otwinowski, Z., and Minor, W. (1997) *Methods Enzymol.* 276, 307–326.
- Navaza, J. (1994) *Acta Crystallogr. A* 50, 157–163.
- Brünger, A. T. (1992) *X-PLOR, A System for X-ray Crystallography and NMR, Version 3.1*, Yale University Press, New Haven, CT.
- Parkinson, G., Vojtechovsky, J., Clowney, L., Brünger, A. T., and Berman, H. M. (1996) *Acta Crystallogr. D* 52, 57–64.

36. Sundaralingam, M., and Biswas, R. (1997) *J. Biomol. Struct. Dyn.* 15, 173–176.
37. Wang, A. H.-J., Fujii, S., van Boom, J. H., van der Marel, G. A., van Boeckel, S. A. A., and Rich, A. (1983) *Nature* 299, 601–604.
38. Lavery, R., and Sklenar, H. (1989) *J. Biomol. Struct. Dyn.* 6, 655–667.
39. Adamiak, D. A., Milecki, J., Popena, M., Adamiak, R. W., Dauter, Z., and Rypniewski, W. R. (1997) *Nucleic Acids Res.* 25, 4599–4607.
40. Westhof, E. (1987) *Int. J. Biol. Macromol.* 9, 186–192.
41. Egli, M., Portmann, S., and Usman, N. (1996) *Biochemistry* 35, 8489–8494.
42. Szymkowski, D. E. (1996) *Drug Discovery Today* 1, 415–428.
43. Akhtar, S., and Agrawal, S. (1997) *Trends Pharmacol. Sci.* 18, 12–19.
44. Antisense '97: A roundtable on the state of the industry (1997) *Nature Biotechnol.* 15, 519–524.
45. Cook, P. D. (1998) in *Protocols in Experimental Pharmacology* (Crooke, S. T., Ed.) Springer, New York (in press).
46. Agrawal, S., Zhang, X., Lu, Z., Zhao, H., Tamburin, J. M., Yan, J., Cai, H., Diasio, R. B., Habus, I., Jiang, Z., Iyer, R. P., Yu, D., and Zhang, R. (1995) *Biochem. Pharmacol.* 50, 571–576.
47. Greig, M. J., Gaus, H., Cummins, L. L., Sasmor, H., and Griffey, R. H. (1995) *J. Am. Chem. Soc.* 117, 10765–10766.
48. Crooke, S. T. (1996) in *Cancer Therapeutics: Experimental and Clinical Agents* (Teicher, B. A., Ed.) pp 299–366, Humana Press, Totowa, NJ.
49. Baker, B. F., Lot, S. S., Condon, T. P., Chen-Flourney, S., Lesnik, E. A., Sasmor, H. M., and Bennett, C. F. (1997) *J. Biol. Chem.* 272, 11994–12000.
50. Takahara, P. M., Frederick, C. A., and Lippard, S. J. (1996) *J. Am. Chem. Soc.* 118, 12309–12321.

BI980392A